METHODOLOGY FOR INDIVIDUAL BLADE CONTROL OF HELICOPTER WITH A DISSIMILAR ROTOR

Beatrice Roget* and Inderjit Chopra†

Alfred Gessow Rotorcraft Center
Department of Aerospace Engineering
University of Maryland, College Park, MD 20742

Abstract

A time domain adaptive control algorithm is developed to reduce hub vibration of a dissimilar rotor. The control strategy can be implemented using smart material actuated on-blade trailing edge flaps. Each flap is controlled individually, optimally taking into account blade dissimilarities and damages. The controller is tested using a comprehensive rotor aeroelastic analysis. The analysis includes dissimilar blade modeling and accounts for aerodynamic and inertial effects of trailing edge flaps. The controller successfully reduces all harmonics of the hub loads arising out of blade dissimilarities. Significant improvements in vibration reduction are predicted using the present individual control method as compared to a classical control method. A 98% reduction is achieved for a single targeted load, and at least 40% for all six hub vibratory loads for a combined objective function. In all cases, trailing edge flap deflections are limited to $\pm 4^{\circ}$.

Notations

C_T	Rotor thrust coefficient
c_m	Section pitching moment coefficient
F_x, F_y, F_z	Fixed frame hub longitudinal, lateral, and vertical shears, non-dimensionalized with respect to $m_{ref}\Omega^2 R^2$
F	Fixed frame hub vibration vector
H	Measurement matrix
I	Identity matrix
J,J_F,J_δ	Scalar non dimensional vibration objective functions
K	Kalman gain vector
M_x, M_y, M_z	Fixed frame hub rolling, pitching and yawing moments, non-dimensionalized with respect to $m_{ref}\Omega^2 R^3$
m_{ref}	Reference mass per unit span
N_s	Number of measurement samples
N_b	Number of blades
P	Covariance of estimation error
Q	Covariance of process noise
r	Covariance of measurement noise
rev	Rotor revolution
R	Rotor radius (dimensional)
T	Transfer matrix relating flap inputs to hub vibration vibration
W_z	Weighting matrix for fixed frame hub loads
W_δ	Weighting matrix for control inputs
$W_{\Delta\delta}$	Weighting matrix for control input rates
x	State vector
z	Measurement vector
δ	Trailing edge flap deflection
$\Delta\delta$	Flap deflection increment in 1 rev
μ	Advance ratio
Ω	Rotor speed (dimensional)
σ	Solidity ratio

Subscripts

j	j^{th} row of a matrix or vector
k	Blade number
l	Hub load number, $l = 1\,to\,6$
n	Iteration number
$()_0$	Uncontrolled

Introduction

Vibration is a serious problem in helicopters and the main rotor is a key source of vibratory loads. Oscillatory air loads are caused by a highly unsteady flow field, complex wake structure, coupled and nonlinear blade motions and time-varying blade pitch inputs. When the blades are identical (tracked rotor), only kN_b/rev harmonic loads occurring at the rotor hub are transmitted to the fuselage (where N_b

*Graduate Research Assistant; student member AIAA, student member AHS.

†Alfred Gessow Professor and Director Alfred Gessow Rotorcraft Center; fellow AIAA, fellow AHS

Presented at the 28th European Rotorcraft Forum, Bristol, U.K., 17-20 September 2002.

is number of blades and k is an integer). On the other hand, if the blades are not identical (dissimilar rotor), significant non-kN_b/rev loads are also transmitted to the helicopter fuselage.

Passive vibration reduction methods like pendulum absorber or modal placement methods have limited effectiveness over a narrow range of flight conditions. The most widely studied active control methods use multicyclic pitch excitation. This method has great potential because it eliminates vibration at its source. This is implemented by actuating the rotor blades at higher harmonics to generate unsteady forces, which when properly phased counteract existing vibratory air loads. Several implementation techniques have been considered, such as HHC (Higher Harmonic Control), IBC (Individual blade Control) and active control of trailing-edge flaps [1].

The HHC technique uses swashplate actuation to control pitch angles of rotor blades. This technique has been demonstrated to reduce vibrations through numerical simulations [2], model and full scale wind tunnel tests [3–5], as well as flight tests of full-scale vehicles [6]. However, this can not control the blades individually. As a result, non kN_b/rev harmonics arising from rotor dissimilarities cannot be controlled.

An extension of this technique uses blade root actuators in the rotating system to individually control each blade pitch (IBC). The potential of this technique to reduce vibration has been demonstrated for identical rotor blades both analytically [7,8] and experimentally [9,10]. Both HHC and IBC methods require a complex actuation system that impose a considerable weight penalty and induce high pitch link loads.

The introduction of smart material actuators has renewed interest for an alternative active vibration control approach that employs trailing-edge flaps [11,12]. These actuators are light weight, high bandwidth, and have low power requirement. Active trailing edge flaps have been shown to achieve a level of vibration reduction comparable with conventional IBC while using moderate input angles [13,14].

The IBC approach, either through complete blade feathering or using trailing-edge flap actuation, allows each blade to be controlled individually and target the non-kN_b/rev loads. However, existing control methodologies do not make use of this capability. They use the same phase-shifted control inputs to all blades, assuming a tracked rotor (identical blades). Dissimilarities in helicopter blades can cause a tremendous increase in vibratory loads at the hub. Currently, to overcome this problem, blade tracking is performed periodically resulting in a significant increase in operating cost. Moreover, to minimize blade dissimilarities, tight manufacturing tolerances are imposed leading to high manufacturing cost. Blade tracking and tight tolerances minimize vibrations, but they are time consuming and expensive.

Recently, closed-loop wind tunnel tests on a 4-bladed Mach scale rotor using piezo-bimorphs actuated trailing edge flaps were conducted in the Glenn L. Martin wind tunnel [15]. This actuation system successfully minimized 4/rev hub loads by over 90% for steady and transient flight conditions. A neural network based time domain adaptive controller was used [16–18]. The controller assumed identical blades. As a result, large 1/rev loads arising out of rotor dissimilarities could not be controlled. Any attempt to target these non-kN_b/rev loads using this controller led to excessive flap requirements. This resulted in saturation of actuators and enormously degraded control performance. The goal of the present study is to develop a new control methodology which takes into account blade dissimilarities and reduces both kN_b and non-kN_b/rev loads.

For the majority of vibration reduction studies, the helicopter is represented by a linear quasi-static frequency domain model, relating input pitch harmonics to the harmonics of output loads [19,20]. For adaptive control strategies, this relation is normally estimated in real time using a Kalman filter identification. This, in conjunction with a quadratic cost function, determines the optimal control inputs for vibration reduction. The controller developed in the present investigation also uses a linear, quasi-static helicopter model, but expressed in time domain. Thus, this model includes all frequencies of both the measured outputs and the control inputs. A similar type study to evaluate a time domain control algorithm was previously reported by the authors [21]. The study was performed on a very simplified blade model undergoing only flapping motion, with uniform inflow distribution. Considerable reductions in vibratory hub loads were predicted in presence of several rotor dissimilarities using control inputs of small amplitude (over 99% reduction of vibratory F_z with 4° peak-to-peak amplitude flap inputs). For this, a simple control strategy to account for rotor dissimilarities was implemented. In this paper, a refined control algorithm to minimize vibratory loads in a dissimilar rotor is presented. The controller performance is investigated using a comprehensive rotor analysis containing flap-lag-torsion motions, free wake modeling and trailing edge flap dynamics.

Helicopter Model

The present comprehensive simulation analysis is based on UMARC (University of Maryland Advanced Rotorcraft Code) [22]. The helicopter is represented by a single main rotor of N_b elastic blades. Each rotor blade is divided into 20 finite elements undergoing flap, lag and torsion degrees of motion. In the present analysis, 4 flap modes, 3 lag modes, and 2 torsion modes are used. Each spatial elements can be modeled with a trailing-edge flap, allowing for an array of independently moving flaps along the blade. The aerodynamic forces on the blade sections containing the flap are obtained assuming changes in the section lift and pitching moment coefficients. Flap inertial effects are included both in the blade equations of motion and in the calculation of hub loads. A bearingless rotor model is used, based on the MD900 helicopter. The model features multiple load paths for the flexbeam/torque tube configuration, viscoelastic snubber, kinematics of control linkage, and non-linear bending-torsion coupling within the flexbeam [23]. The characteristics of the model rotor are presented in Table 1. A refined pseudo-implicit free wake model developed by Bagai and Leishman [24] is incorporated in the analysis.

The rotor is first trimmed to zero first harmonic flapping and a target C_T/σ. The shaft angle is adjusted to provide propulsive trim. The controller is then activated. The analysis calculates the steady state hub loads resulting from a given flap input. Based on these hub loads, the flap inputs are updated every rotor revolution. The blade hub loads resulting from the flap actuation are calculated in the rotating frame for each blade by integrating the blade inertial and aerodynamic sectional loads. The rotating system blade loads are then transformed to the fixed frame. If the N_b blades are identical, only the loads at integer multiple of N_b/rev appear in the fixed frame. If the blades are dissimilar, all harmonics appear in the fixed frame.

Control Algorithm

A control algorithm is required to determine optimal control input for each blade. Different control inputs respectively generated for each blade can attempt to minimize both the baseline kN_b/rev vibration and the dissimilarity-induced non-kN_b/rev loads.

The linear quasi-static model relating the response vector F to the multicyclic pitch vector δ through a transfer function is described as :

$$F = F_0 + T\,\delta \tag{1}$$

F is a vector representing the fixed system hub loads sampled over one rotor revolution at N_s azimuthal points; F_0 represents the uncontrolled fixed system hub forces and moments; δ is a vector containing the N_b individual flap inputs, and T is a $(6N_s)\times(N_bN_s)$ transfer matrix. Note that this model assumes that the fixed system hub loads are periodic. For a 5-bladed rotor, Eq. (1) can be written as:

$$\begin{Bmatrix} F_x \\ F_y \\ F_z \\ M_x \\ M_y \\ M_z \end{Bmatrix} = \begin{Bmatrix} F_{x0} \\ F_{y0} \\ F_{z0} \\ M_{x0} \\ M_{y0} \\ M_{z0} \end{Bmatrix} \cdots + \begin{bmatrix} T_{11} & T_{12} & T_{13} & T_{14} & T_{15} \\ T_{21} & T_{22} & T_{23} & T_{24} & T_{25} \\ T_{31} & T_{32} & T_{33} & T_{34} & T_{35} \\ T_{41} & T_{42} & T_{43} & T_{44} & T_{45} \\ T_{51} & T_{52} & T_{53} & T_{54} & T_{55} \\ T_{61} & T_{62} & T_{63} & T_{64} & T_{65} \end{bmatrix} \begin{Bmatrix} \delta_1 \\ \delta_2 \\ \delta_3 \\ \delta_4 \\ \delta_5 \end{Bmatrix} \tag{2}$$

The fixed system hub loads are numbered from 1 to 6 in the order shown in Eq. (2). Each transfer matrix T_{lk} is a $(N_s)\times(N_s)$ matrix relating the l^{th} hub load F_l to the flap input δ_k to blade k. In the case of perfectly identical blades, for any load F_l, there exists a relationship between the transfer matrices T_{lk} and T_{lk+1}:

$$T_{lk+1} = S\,T_{lk} \tag{3}$$

where S is a matrix operator that permutes the

Table 1 MD-900 rotor characteristics

Parameters	Symbol	Value
Number of blades	N_b	5
Rotor radius	R	16.925 ft
Rotor speed	Ω	392 RPM
Chord (nominal)	c/R	0.0492
Lock number (nominal)	γ	9.17
Solidity	$N_bc/\pi R$	0.0779
Lift curve slope	c_1	7.10
Lift coefficient at $\alpha = 0$	c_0	0.1123
Pitching moment coefficient	c_{mac}	-0.008
Flap spanwise location / R	r_{mid}	0.83
Flap chord / nominal chord	c_f	0.25
Flap length / R	l_f	0.18
Twist	θ_{tw}	10°
Reference mass/span	m_{ref}	0.0655 slug/ft
Reference shear	$m_{ref}\Omega^2R^2$	31,600 lb
Reference moment	$m_{ref}\Omega^2R^3$	535,000 ft-lb

transfer matrix rows:

$$S = \begin{bmatrix} 0 & I_p \\ I_q & 0 \end{bmatrix} \tag{4}$$

with $p = (N_b - 1)\,\frac{N_s}{N_b}$ and $q = \frac{N_s}{N_b}$.

Using this global model, the identification problem involves determination of the transfer matrix, given the control inputs and measured vibration outputs. The transfer matrix varies with helicopter operating conditions (e.g., thrust, airspeed). Therefore, the identification method should be made online to track the transfer matrix in real-time. In the present study, the Kalman filter method is used. It is a computationally efficient algorithm designed to update parameter estimates recursively on the basis of a single measurement. Although the uncontrolled vibration vector F_0 can be obtained from measurements with no flap control inputs, it should be estimated along with the transfer matrix T because it will vary with flight conditions and helicopter characteristics. Eq. (1) can then be rewritten as:

$$F = [TF_0] \begin{Bmatrix} \delta \\ 1 \end{Bmatrix} \tag{5}$$

At any iteration n, the typical form for the j^{th} measurement is (measurement model):

$$\begin{aligned} (F_j)_n &= [\delta_n\ 1] \begin{Bmatrix} (T_j)_n^T \\ (F_{0j})_n \end{Bmatrix} \\ &= H_n\, x_n + v_n \\ &= z_n \end{aligned} \tag{6}$$

where (T_j) is the j^{th} row of T. Following the notations used in Ref.[25], z_n is the measurement vector, x_n is the state vector to be estimated, and H_n represents the measurement matrix. The measurement noise v_n is also included in the measurement model, and is assumed to be a zero-mean, white sequence of constant covariance r. For simplicity, the subscript j is omitted in these notations. Because the loads are periodic and sampled over one rotor revolution, the state vector dynamics (system model) is assumed quasi-static and is written as:

$$x_n = x_{n-1} + w_{n-1} \tag{7}$$

where w_{n-1} is the process noise, assumed to be a zero-mean, white sequence of constant covariance Q. Based on the measurement and system models, the Kalman filter discrete equations for updating state estimates are written as:

$$\begin{aligned} &Kalman\,gain\,matrix: \\ &K_n = P_{n-1}{H_n}^T \left[H_n P_{n-1} {H_n}^T + r\right]^{-1} \end{aligned} \tag{8}$$

$$\begin{aligned} &Error\,covariance\,update: \\ &P_n = [I - K_n H_n]\,[P_{n-1} + Q] \end{aligned} \tag{9}$$

$$\begin{aligned} &State\,estimate\,update: \\ &x_n = x_{n-1} + K_n\,(z_n - H_n x_{n-1}) \end{aligned} \tag{10}$$

Note that the Kalman gain vector K_n is same for all j measurements, so that the unknown parameters $[TF_0]$ can be identified in a single step:

$$[TF_0]_n = [TF_0]_{n-1} + \left(F_n - [TF_0]_{n-1} \begin{Bmatrix} \delta_n \\ 1 \end{Bmatrix}\right) {K_n}^T \tag{11}$$

This represents an important reduction in computation time since P_n and K_n are calculated only once for each time-cycle, and the computation of K_n only requires inversion of a scalar. Once the state estimates are obtained, the optimal control inputs can be determined. In the present investigation, a deterministic controller is used. For this controller, all the model properties are known from the identification algorithm. The individual multicyclic controls are based on the minimization of the performance function J, expressed as:

$$\begin{aligned} J &= J_F + J_\delta \\ J_F &= Y^T W_F Y \\ J_\delta &= \delta^T W_\delta \delta + \Delta\delta^T W_{\Delta\delta} \Delta\delta \\ where\ Y &= F - (F_0)_{mean} \end{aligned} \tag{12}$$

For simplicity, the subscript n indicating the iteration number is omitted. The weighting matrices W_F, W_δ, and $W_{\Delta\delta}$ are applied to the output response, the individual flap input controls, and the individual flap control rates, respectively. Typically, these are diagonal matrices. Some diagonal elements of W_F can be set to zero to keep the corresponding vibration component uncontrolled. W_δ limits the flap control amplitude, and $W_{\Delta\delta}$ limits the control rate. In the present report, $W_{\Delta\delta} = 0$, but a hard limit $\Delta\delta_{max}$ is imposed on $\Delta\delta$ at each time-cycle to prevent large control variations. The optimal control input for each blade is obtained from the minimization of the performance function J, which means $\partial J/\partial\delta = 0$. This results in the optimal control solution in the form (for $W_{\Delta\delta} = 0$):

$$\begin{aligned} \left(\delta^{opt}\right)_n &= -DT^T W_F Y_n \\ where\ D &= \left[T^T W_F T + W_\delta\right]^{-1} \end{aligned} \tag{13}$$

Note that the control vector δ contains the individual inputs for each trailing edge flap. This means that if the blades are dissimilar, the control inputs to each blade will differ, even in the case where only one blade is damaged. In a previous study [21], a more

intuitive control strategy was used whereby only the control input corresponding to the damaged blade was different. This added constraint resulted in higher control angles than the more general method presented here.

Results

Controller performance is investigated under wind tunnel trim conditions at $\mu = 0.2$, $C_T/\sigma = 0.075$ and a forward shaft tilt angle of 5°. To simulate measurements, $N_s = 60$ samples are used for each rotor revolution. To initialize the system identification procedure, a value is chosen for the system noise covariance matrix Q, and the measurement noise covariance r (scalar). Initial guesses are also made for the state vector x_0 and estimate error covariance matrix, P_0. $x_0 = 0$, $P_0 = I_{(N_b N_s+1)}$, $Q = 10^{-5}.I_{(N_b N_s+1)}$, and $r = 10^{-5}$ are chosen. For the controller, a hard limit of $\delta_{max} = \pm 4°$ is always imposed on the flap deflection, and $\Delta\delta_{max}$ is adjusted to avoid large transient hub loads.

First the transfer matrices relating the flap control inputs to hub loads are identified. Then the performance of the controller with identical rotor blades (baseline) is described. Next, the effect of rotor dissimilarities on the hub vibration is determined. Finally, the controller performance for reducing hub vibration with dissimilar rotor is investigated. Comparison is made with a classical controller that does not account for blade dissimilarities.

In a second stage, controller performance is investigated under wind tunnel trim conditions at advance ratios from $\mu = 0.10$ to $\mu = 0.40$, with $C_T/\sigma = 0.075$. The present individual control method is compared with a classical controller.

Transfer matrix identification

First, the transfer matrix relating the flap control inputs to the fixed system hub forces and moments is identified. Results are shown for the baseline rotor. A representation of the transfer matrices, T_{l1}, ($l = 1\,to\,6$, Eq. 2) for blade 1 is shown in Figure 1. The columns are plotted versus azimuth for one rotor revolution. Each column vector represents the hub force or moment resulting from an impulsive unit flap input, at a particular azimuth, for a specific blade. For example, the curves highlighted in white in Figure 1 are the 16th columns of matrices T_{l1}, $l = 1, 6$. They correspond to the fixed frame hub forces and moments resulting from an impulsive input of amplitude 1° at $\Psi = 90°$ (with $N_s = 60$), to blade 1.

Figure 1 shows that the longitudinal and lateral hub shears are much less sensitive to flap actuation

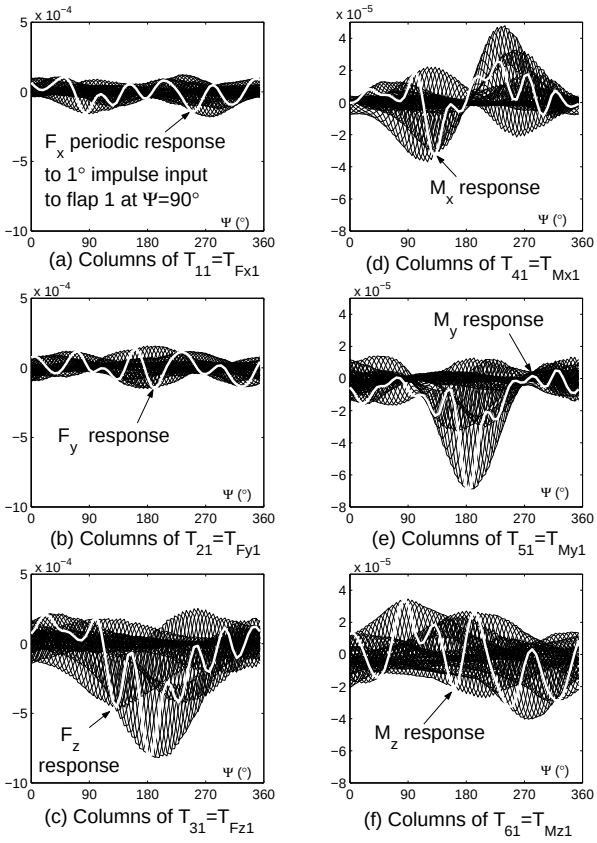

Fig. 1 Representation of input/output transfer matrix for blade 1 (baseline rotor, $\mu = 0.2$)

than the vertical hub shear (about 3.5 times less sensitive). On the other hand, the three hub moments have comparable sensitivities to the flap deflection. Sensitivity results obtained with the damaged rotor are very similar.

Control of baseline rotor

The closed-loop control is then applied to the rotor model to reduce hub vibration through optimal flap inputs. In the first stage, the weighting matrix W_F is adjusted to control only one fixed system hub load at a time. The optimal control inputs reach convergence after about 150 rotor revolutions. Results are shown in Figures 2 and 4. Figure 2 shows the effect of the optimal flap actuation on all fixed system hub loads when the controller attempts to reduce one particular load. The uncontrolled and controlled peak-to-peak amplitude are represented for each hub load (non-dimensionalized as shown in Table 1). For every one of six cases, the reduction of considered hub load is over 98%. However there are significant increases in other vibratory components. This is especially true when the objective to minimize F_x or F_y is implemented; the vibration amplitudes for the vertical hub shear and yawing

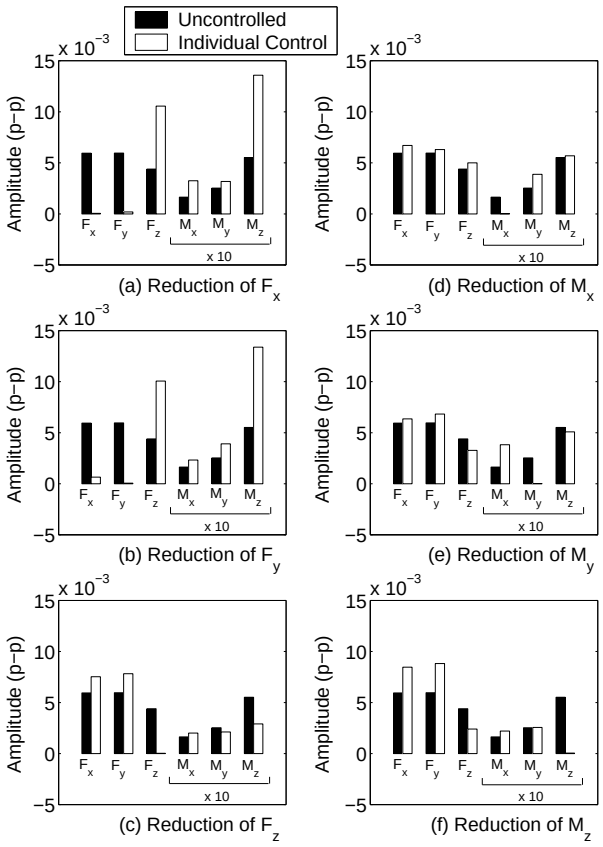

Fig. 2 Controller performance to reduce each hub load separately (baseline rotor, $\mu = 0.2$)

moment are more than doubled. On the contrary, reducing of F_x also results in the reduction of oscillatory F_y, and vice versa. The reduction of F_z, M_x, or M_y has a relatively small detrimental effect on F_x and F_y vibration. The reduction of M_x leads to an increased M_y vibration, and vice versa. On the contrary, reducing the vertical shear F_z also results in a decreased vibratory hub yawing moment, and vice versa. These observations are summarized in Figure 3, where a dashed line signifies a detrimental effect and a continuous line indicates a beneficial effect between two loads. Note that the detrimental effects are equally present in classical control and are not artifacts of the individual control algorithm.

Figure 4 shows both the amplitude and phase of the flap control inputs required to reduce each hub load. Note that this is still for the baseline rotor with identical blades, therefore the optimal input is identical for all blades. As shown by the transfer matrices in Figure 1, we observe that the largest flap deflection is needed for the reduction of the hub shears F_x and F_y (about 2° peak-to-peak). For all other loads, the deflection amplitude is comparably small, about 1° peak-to-peak. The most important flap harmonics, i.e. 4/rev, 5/rev and 6/rev for the 5-bladed rotor, are shown in shades of grey, whereas other harmonics are shown in white. Note that even though these three harmonics are dominant, actuating the flaps at other frequencies also contributes towards vibration reduction. In particular, the 7/rev and 8/rev flap components seem to be important for the reduction of the hub vibratory moments M_x and M_y. The 2/rev and 3/rev components are also relatively important when the objective is to minimize the oscillatory inplane shear F_x or F_y. The flap deflections required for minimizing F_x or F_y are very similar qualitatively, with large 4/rev and 5/rev components. Flap inputs corresponding to the reduction of F_z or M_z, have 5/rev as the dominant frequency. Flap inputs necessary to reduce M_x or M_y also appear qualitatively similar, with the 6/rev as dominant harmonic. However, Figure 4(b) shows that the phases of the 6/rev harmonic components are opposite to each other. These are in agreement with the relations shown in Figure 3.

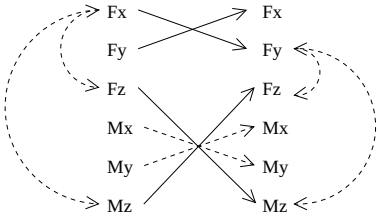

Fig. 3 Multiple load vibration reduction: interaction between loads

In the second stage, simultaneous reduction of all loads is attempted. Weights are adjusted for each load to give them comparable importance in the objective function. Results are shown in Figure 5. Contrary to the previous single load control cases, it is not possible to reduce completely all six vibratory loads simultaneously. The vibration is reduced by more than 80% for three hub loads and over 60% for other three hub loads. The flap deflection required to achieve this is considerably increased while still remaining within limits of $\pm 4^\circ$. The 3/rev component is the dominant flap input.

Effect of rotor dissimilarity

Rotor dissimilarities are introduced by modeling rotor faults. Two types of rotor faults are considered. The first fault is simulated by increasing the mass of the blade section corresponding to the trailing-edge flap in blade 1 by 1%. The second fault is simulated by increasing the nose-down pitching moment coefficient for the same section from $c_m = -0.008$ to $c_m = -0.01$. The trailing edge flaps, of chord $c_f = 25\%$ of nominal blade chord, extend from $0.74R$ to $0.92R$ for each blade.

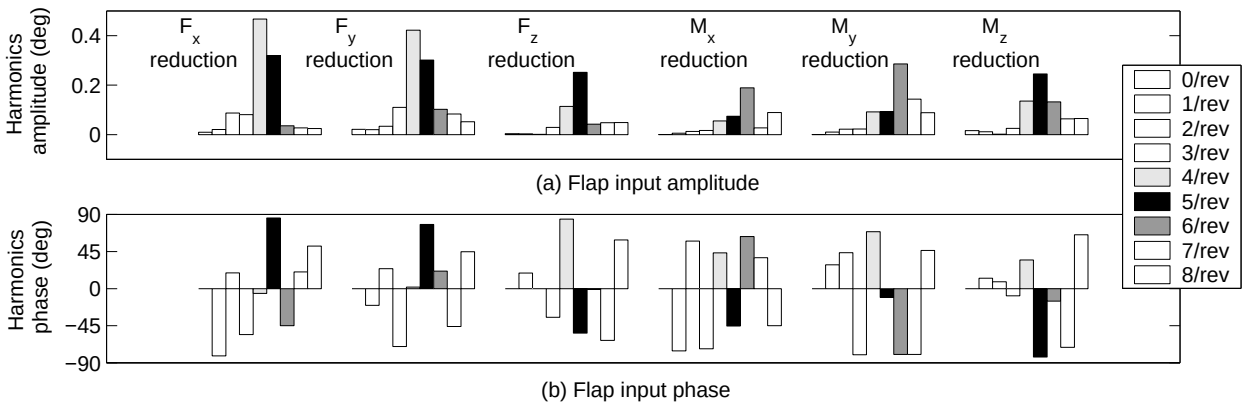

Fig. 4 Optimal flap inputs required to reduce each hub load separately (baseline rotor, $\mu = 0.20$)

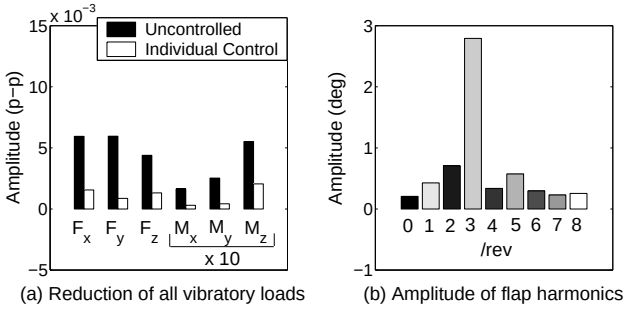

Fig. 5 Simultaneous vibration reduction of all hub loads (baseline rotor, $\mu = 0.2$)

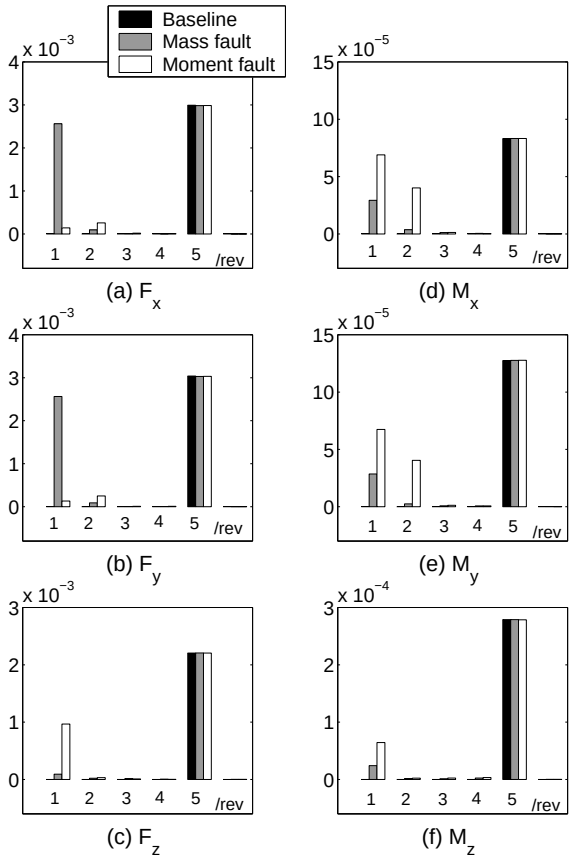

Fig. 6 Effect of rotor faults on magnitude of hub loads harmonics ($\mu = 0.2$)

Figure 6 shows the magnitude of harmonics for the six fixed system hub loads, in the case of baseline and damaged rotor. Only the first five harmonics are shown, since the amplitudes of harmonics higher than 5/rev are negligible. For the baseline rotor, only 5/rev component is present for this 5-bladed rotor. Even though the extent of damage is very small, there is a significant effect on other vibratory harmonics. The mass damage introduces a large 1/rev component in the lateral and longitudinal hub shears. A moderate 1/rev vibration is also present in the rolling and pitching moments. The effect on the vertical hub shear and the yawing moment is small. By contrast, the effect of the aerodynamic damage is more significant on the rolling and pitching moments, especially as 1/rev and 2/rev components. It also introduces a 1/rev component in vertical shear. Unlike the mass damage, the increase in 1/rev lateral and longitudinal hub vibration due to moment fault is not significant.

Control of dissimilar rotor

The performance of the present controller (individual control) is now tested with dissimilar blades and compared to that of a controller using identical flap inputs (classical control). For classical control, the objective function only includes the kN_b/rev harmonics.

First, the mass fault is simulated in blade 1. Figure 7 presents the vibration reduction achieved when the objective function consists of only one hub load, using classical control and refined individual control. Using the present controller, the considered oscillatory load is reduced in all six cases by more than

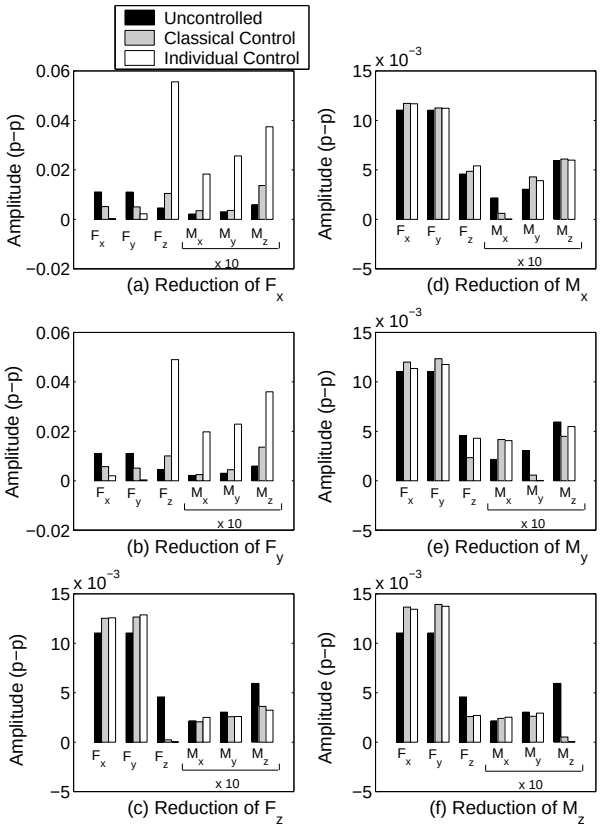

Fig. 7 Controller performance to reduce each hub load separately (mass fault in blade 1, $\mu = 0.2$)

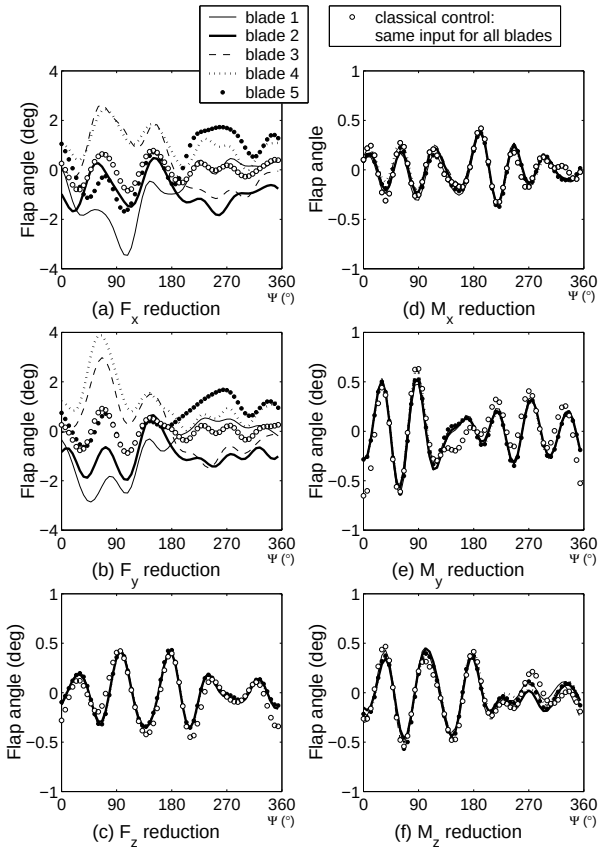

Fig. 8 Optimal angles required to reduce each hub load separately (mass fault in blade 1, $\mu = 0.2$)

98% in amplitude. However, the reduction of either F_x or F_y causes a dramatic increase in all other hub loads. The classical controller is unable to reduce either F_x or F_y vibration by more than 50%. This is because only the 5/rev harmonics is reduced: this controller has no effect on the 1/rev component, which is very large in F_x and F_y for the mass damage. Figure 8 shows the corresponding optimal control inputs. Because the blades are dissimilar, the controller now generates different flap inputs for each blade. Flap deflections required for minimizing either F_x or F_y show large variations from one blade to another. These variations translate into non-kN_b/rev loads in the fixed frame. These non-kN_b /rev counteract the large 1/rev components of F_x and F_y. On the contrary, the flap inputs generated for the reduction of other loads are similar for all blades. This is because the non-kN_b/rev harmonics are relatively small for these loads. In Figure 8, the optimal control input required for all blades using classical control is also shown. As expected, the inputs required using the classical method and the individual control method are different when the targeted hub load contains significant non-kN_b/rev

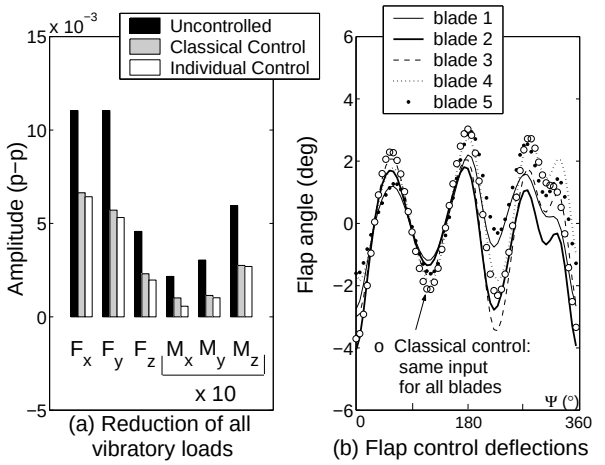

Fig. 9 Simultaneous control of all hub loads (mass fault in blade 1, $\mu = 0.2$)

harmonics.

The objective function is then modified to attempt reducing all fixed system hub loads simultaneously. Figure 9 shows the vibration reduction achieved and the flap control inputs required. The maximum

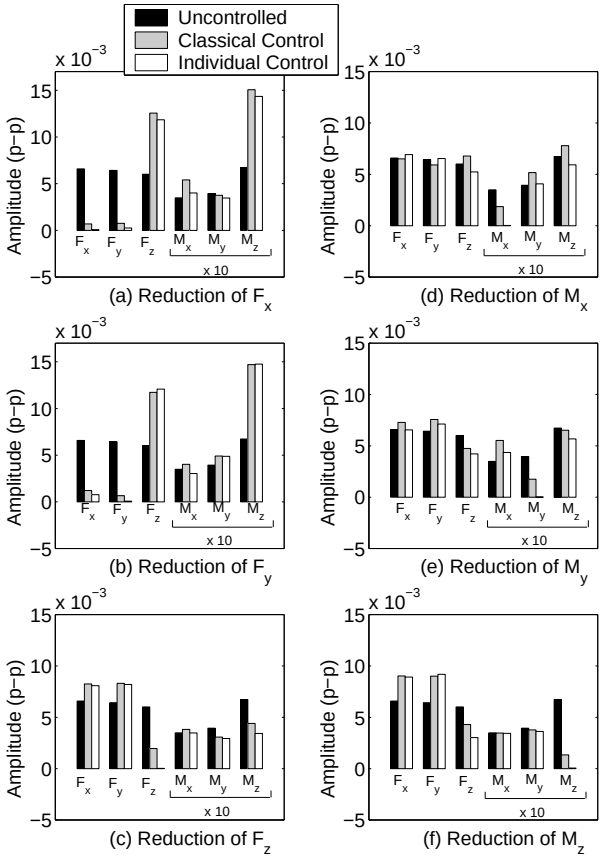

Fig. 10 Controller performance to reduce each hub load separately (aerodynamic fault in blade 1, $\mu = 0.2$)

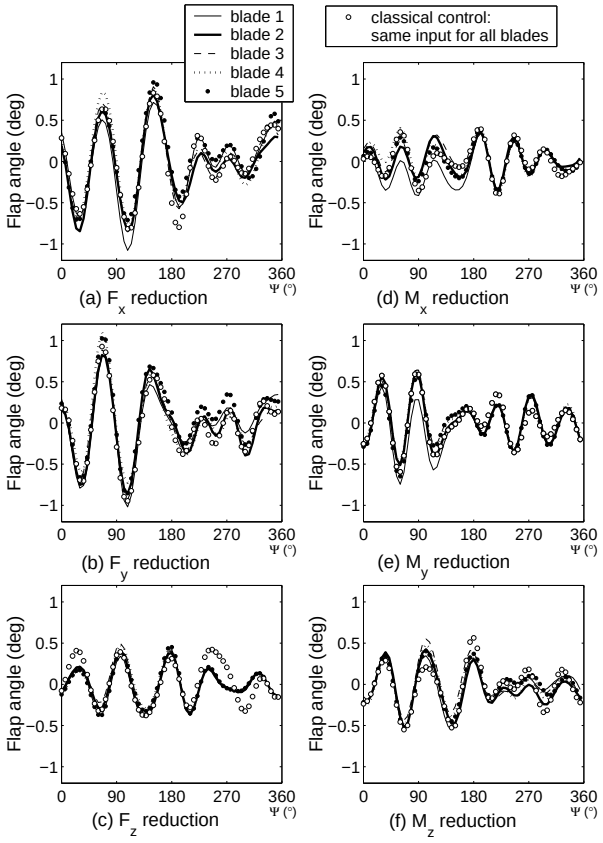

Fig. 11 Optimal angles required to reduce each hub load separately (aerodynamic fault in blade 1, $\mu = 0.2$)

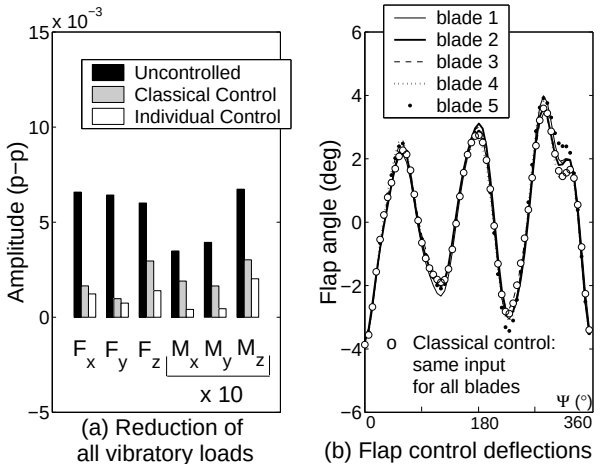

Fig. 12 Simultaneous control of all hub loads (aerodynamic fault in blade 1, $\mu = 0.2$)

flap deflection of 4° is needed while only 40% reduction in vibratory amplitude for F_x is achieved. Note that the 3/rev harmonic is again dominant in the flap inputs for all blades. For this mass damage, the advantage of using individual flap inputs is less appealing. Vibrations can be reduced completely for each load separately but at the cost of increasing vibrations for other hub loads. For simultaneous control of all loads, individual control performance is only slightly improved compared to classical control. Inability of the individual controller to further reduce the hub vibrations stems from actuator saturation. Higher flap deflections will lead to better control. With flap deflection limited to ±6°, at least 60% vibration reduction is achieved for all loads. Performance of the classical controller, on the other hand, is inherently limited by its inability to reduce non-kN_b/rev vibrations. As a result, increasing the maximum flap deflection does not improve controller performance. Actuator saturation is caused by the following three reasons. The greatest effect of mass damage is felt in F_x and F_y vibrations. The sensitivity of F_x and F_y to flap deflections is small. The effect of reducing either F_x or F_y vibrations is detrimental for all other vibratory loads.

The aerodynamic pitching moment dissimilarity introduces significant 1 and 2/rev components in M_x and M_y. Also a large 1/rev component is induced

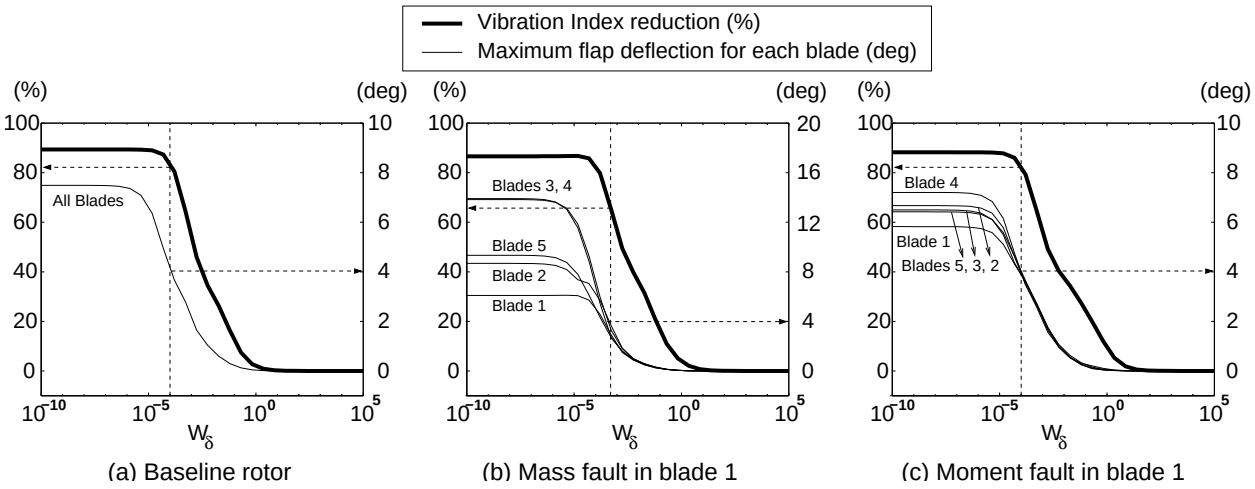

Fig. 13 Effect of varying the weight applied to flap inputs

in F_z. However the effect on F_x or F_y is small. Figure 10 shows the vibration reduction achieved when the objective function contains only one hub load. Figure 11 shows the corresponding flap deflections. Figure 10 shows that each load can be separately reduced by more than 98% using individual control. Using classical control, the pitching and rolling moment vibration is reduced by only 50% while the vertical vibration is reduced by 60%. The large non-kN_b/rev components present in these vibratory loads can not be controlled using identical flap inputs. Note that the corresponding optimal flap inputs (Figure 11) are very similar for both methods. Hence vibration reduction can be improved without any increase in flap deflections, simply by using slightly different inputs for each flap. All loads are reduced separately with flap deflections less than 2° peak-to-peak.

Finally simultaneous reduction of all six hub loads in presence of pitching moment dissimilarity is described. The results are shown in Figure 12. Using individual control all loads are reduced by more than 70%. This is higher than the reduction achieved by classical control. The required flap deflections are similar for all blades, with a dominant 3/rev component and about 4° half peak-to-peak amplitude. Again, it is observed that small variations in deflection from flap to flap can result in greatly improved vibration reduction.

Effect of control input weight

Figure 13 shows the effect of varying the control input weight on the controller performance. The controller performance is measured by the vibration reduction (with vibration index defined as $\sqrt{J_F}$) as well as the maximum flap deflections. Three cases are considered: baseline rotor, rotor with mass fault in one blade, and rotor with aerodynamic fault in one blade. The control objective is to reduce all loads simulateously.

Previous results (Figures 5, 10, and 13) are indicated by the dashed lines. For these results, the weighting matrices W_δ have been chosen such that the maximum flap deflection is 4°. For the baseline rotor as well as for damaged rotor, the maximum vibration reduction that can be achieved is about 88%. However, for the baseline rotor, flap deflections are identical for all blades, while for the damaged rotor, they are different. The maximum flap deflection required for baseline rotor is about 7.5°.

The flap deflections required for the rotor with a mass fault are much larger, up to 14°. However, when these deflections are limited to 4°, the vibration index is still reduced by about 65%. Note that a small increase in maximum flap deflection (e.g., from 4° to 6°) would result in greater vibration reduction (from 65% to 80%).

The flap deflections required for the rotor with a moment fault are very similar to the baseline rotor case (about 7.5°). Note that because this damage is simulated by a change in pitching moment for the blade section corresponding to the flap, it is also possible to cancel the vibration caused by this fault by imposing a steady deflection to this flap. However this steady input needs to be added to the input required for cancelling the baseline vibration. Finally the total maximum flap deflection would be larger than that computed by the controller.

Effect of advance ratio

The controller performance is now tested at different advance ratios for the baseline and the damaged rotor. The objective function includes only the fixed system hub shears F_x, F_y and F_z, with re-

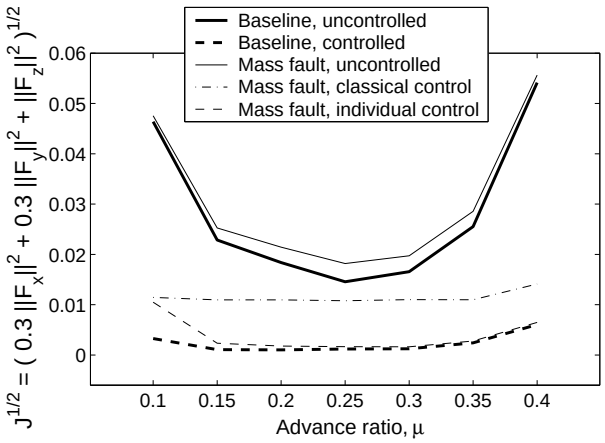

(a) Vibration Index with and without control

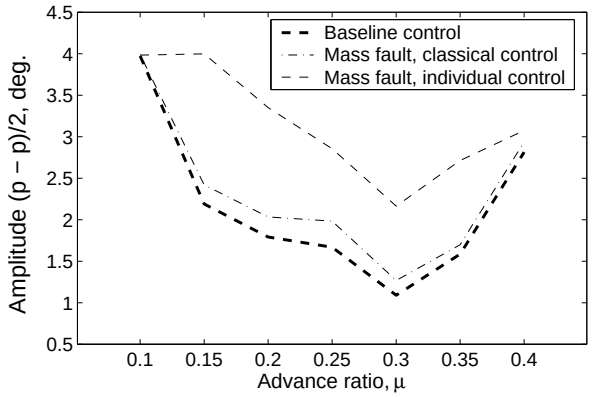

(b) Maximum half peak–to–peak flap deflection

Fig. 14 Vibration index with and without control and required flap deflection for baseline rotor and rotor with mass fault in blade 1.

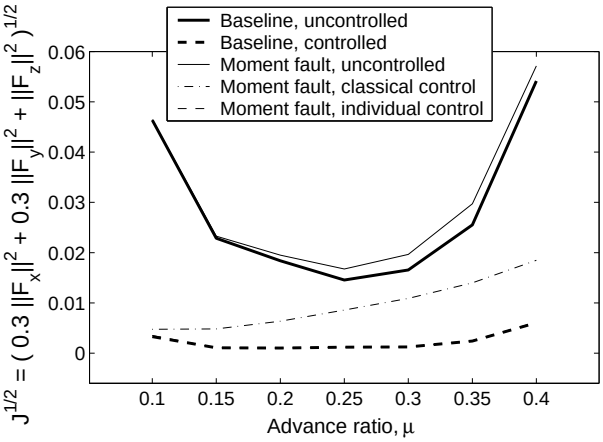

(a) Vibration Index with and without control

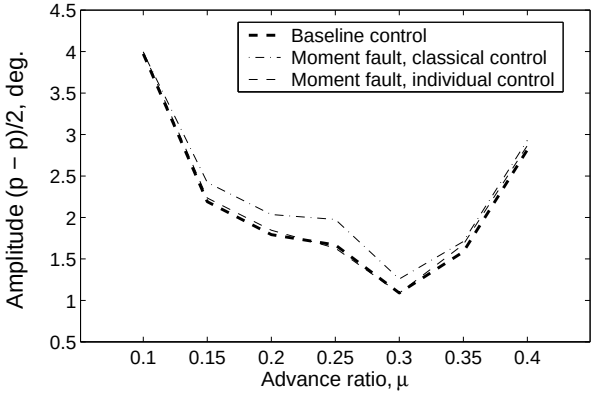

(b) Maximum half peak–to–peak flap deflection

Fig. 15 Vibration index with and without control and required flap deflection for baseline rotor and rotor with moment fault in blade 1.

spective weights of 0.3, 0.3 and 1, chosen so that each load has comparable importance in the objective function at $\mu = 0.20$. Figure 14(a) shows the vibration index $\sqrt{J_F}$ for the baseline rotor and the rotor with a mass fault in blade 1, with and without control. The performance of a classical controller is also shown. Figure 14(b) represents the half peak-to-peak flap deflections. The vibration index is minimum at $\mu = 0.25$. It increases at low advance ratio ($\mu = 0.10$) and high advance ratio ($\mu = 0.40$). The mass fault introduces large 1/rev component in the F_x and F_y shears, while the effect on F_z is very small. The increase in vibration is almost constant at all advance ratios for this mass damage. As a result, the relative increase in vibration is the greatest at moderate advance ratios (low vibration). For the baseline rotor, the vibration index $\sqrt{J_F}$ is reduced by more than 88% at all advance ratios, and up to 95% at $\mu = 0.20$. The flap deflection required is smaller than 4° half peak-to-peak, and about 1° half peak-to-peak at $\mu = 0.30$.

For the damaged rotor with a mass fault in blade 1, the individual control method is compared with the classical controller. Using individual control, the vibration reduction achieved is very close to the baseline results for $\mu \geq 0.15$. However, the required flap deflection are larger (about 2.2° half peak-to-peak at $\mu = 0.30$). For $\mu \leq 0.15$, the 4° limit is reached, resulting in less vibration reduction. For example, at $\mu = 0.10$, the vibration index is reduced by 78% using this limited flap deflection. Using classical control, the flap deflection is smaller. However, the vibration cannot be reduced by more than 75%, and as low as 40% at $\mu = 0.25$. This is because the non-kN_b/rev vibration can not be reduced using identical inputs for all blades. Note that since this vibration component is almost constant at all advance ratios, the reduced vibration index using classical control is also constant for all advance ratios.

Figure 15(a) and 15(b) shows the vibration index $\sqrt{J_F}$ and flap deflections for the baseline rotor

and the rotor with the aerodynamic moment fault in blade 1, with and without control. Contrary to the mass fault case, the vibration increase due to the moment fault becomes larger at higher advance ratios. Figure 15(a) shows that using individual control, it is possible to achieve the same level of vibration reduction as for the baseline rotor. Moreover, Figure 15(b) shows that the required flap deflections are very close to the baseline rotor case; smaller than 4° half peak-to-peak at all advance ratios, and about 1° half peak-to-peak at $\mu = 0.30$. However, using classical control, it is not possible to control the non-kN_b/rev vibration caused by the moment damage (Figure 15(a)). Since this additional vibration increases with advance ratio, the performance of the classical control deteriorates at higher advance ratios. At $\mu = 0.10$, the vibration index can be reduced almost as well as for the baseline rotor (about 90% reduction). However, at $\mu = 0.30$, only 45% reduction can be achieved. This clearly illustrates the advantage of using different inputs for each blade: at $\mu = 0.30$, the vibration reduction can be increased from 45% to 94%, with smaller flap deflections.

Summary and Conclusions

The performance of a new control algorithm to reduce helicopter hub vibrations using trailing edge flaps has been investigated. This new controller takes into account rotor dissimilarities and allows different control inputs to be applied to each trailing edge flap. A comprehensive analytic model based on a modern bearingless rotor was used in numerical simulation. The controller performance was tested at advance ratios from $\mu = 0.10$ to $\mu = 0.40$, both for the baseline rotor with identical blades and the damaged rotor with dissimilar blades. The new controller was compared to a classical controller which uses identical inputs for all trailing edge flaps. The rotor faults were modeled as changes in inertial and aerodynamic properties for the damaged blades. Observations from the present study are as follows:

1. Longitudinal and lateral hub shears are about 3.5 times less sensitive to trailing edge flap deflections than other loads. For the baseline rotor, each hub vibratory load can be separately reduced by more than 98% using moderate flap inputs (1° half peak-to-peak at $\mu = 0.20$). For simultaneous control of all loads, reductions of more than 60% are achieved for all loads using flap inputs of amplitude 4° half peak-to-peak.

2. A small mass fault adds a large 1/rev harmonic in the longitudinal and lateral hub shears. In this case too, all hub vibratory loads can be separately reduced by more than 98% with flap inputs less than ±4° at $\mu = 0.20$. However in the case of the longitudinal and lateral hub shears, such dramatic vibration reduction is accompanied by very large increases in other loads (up to 12 times). When controlled simultaneously, all loads are reduced by at least 40%. This is only slightly better than the performance of a classical controller. This is because the limit of ±4° imposed on the flap deflection is reached.

3. The aerodynamic fault introduces significant 1/rev and 2/rev components in the hub rolling and pitching moments, as well as a large 1/rev harmonic in the vertical hub shear. Again, all hub vibratory loads can be separately reduced by more than 98%, with moderate flap inputs (1° half peak-to-peak at $\mu = 0.20$). When controlled simultaneously, all loads are reduced by more than 70%. This represents a significant improvement compared to the performance of the classical controller (50%).

4. The vibration increase caused by the mass damage is almost constant with advance ratio, while the vibration increase caused by the moment damage becomes larger at higher advance ratios. Significant improvements in vibration reduction are predicted for all advance ratios from $0.10 \leq \mu \leq 0.40$ using the present individual control method as compared to a classical control method. At $\mu = 0.30$, the vibration index reduction is increased from less than 45% to more than 90% using less than 2.5° half peak-to-peak flap deflections for both the structural and aerodynamic faults.

Acknowledgements

The authors gratefully acknowledge the support for this research work provided by the Army Research Office under grant DAAH-04-96-10334, Technical Monitor, Dr. Gary Anderson, and the Boeing company, Technical monitor, Dr. Friedrich Straub.

References

[1]Friedmann, P.P., and Millott, T.A., "Vibration Reduction in Rotorcraft Using Active Control: A Comparison of Various Approaches", *Journal of Guidance, Control, and Dynamics*, Vol 18,(4), July-August 1995.

[2]Nguyen, K., and Chopra, I., "Application of Higher Harmonic Control to Rotors Operating at High Speed and Thrust", *Journal of the American Helicopter Society*, Vol 35,(3), 1990.

[3]Hammond, C. E., "Wind Tunnel Results Showing Rotor Vibratory Loads Reduction Using Higher Harmonic Blade Pitch", *Journal of the American Helicopter Society*, Vol 28,(1), January 1983.

[4]Shaw, J., Albion, N., Hanker, E.J., and Teal, R.S., "Higher Harmonic Control: Wind Tunnel Demonstration of Fully Effective Vibratory Hub Forces Suppression", *Journal of the American Helicopter Society*, Vol 34,(1), January 1989.

[5]Nguyen, K., Betzina, M., and Kitaplioglu, C., "Full-Scale Demonstration of Higher Harmonic Control for Noise and Vibration Reduction on the XV-15 Rotor", *Journal of the American Helicopter Society*, Vol 46,(3), July 2001.

[6]Wood, E.R., Powers, R.W., Cline, C.H., and Hammond, C.E., "On Developing and Flight Testing a Higher Harmonic Control System", *Journal of the American Helicopter Society*, Vol 30,(1), January 1985.

[7]Ham, N.D., "Helicopter Individual Blade Control and its Applications", American Helicopter Society 39th Annual Forum, St. Louis, MO, May 1983.

[8]Guinn, K.F., "Individual Blade Control Independent of a Swashplate", *Journal of the American Helicopter Society*, Vol 27,(3), July 1982.

[9]Richter, P., and Blaas, A., "Full Scale Wind Tunnel Investigation of an Individual Blade Control System for the BO-105 Hingeless Rotor", 19th European Rotorcraft Forum, Cernobbio, Italy, September 1993.

[10]Jacklin, S. A., and Nguyen, K., Blaas, A., and Richter, P., "Full-Scale Wind Tunnel test of a Helicopter Individual Blade Control System", American Helicopter Society 50th Annual Forum, Washington, DC, May 1994.

[11]Chopra, I., "Status of Application of Smart Structures Technology to Rotorcraft Systems", *Journal of the American Helicopter Society*, Vol 45,(4), October 2000.

[12]Straub, F.K., "A Feasibility Study of Using Smart Materials for Rotor Control", *Smart Materials and Structures*, Vol 5,(1), February 1996.

[13]Millott, T.A., and Friedmann, P.P., "Vibration Reduction in Helicopter Rotors Using an Active Control Surface Located on the Blade", 33rd AIAA/ASME/ASCE/AHS/ASC Structures, Structural Dynamics and Materials Conference, Dallas, TX, April 13-15, 1992.

[14]Milgram, J., and Chopra, I., "Parametric Design Study for Actively Controlled Trailing Edge Flaps", *Journal of the American helicopter Society*, Vol 43,(2), 1998.

[15]Koratkar, N.A., Spencer, M.G., and Chopra, I., "Wind Tunnel Testing of a Mach-Scaled Active Rotor with Trailing-Edge Flaps", American Helicopter Society 57th Annual Forum, Washington, DC, May 2001.

[16]Spencer, M.G., Sanner, R.M., and Chopra, I., "Adaptive Neurocontrol of Simulated Rotor Vibrations Using Trailing Edge Flaps", *Journal of Intelligent Material Systems and Structures*, Vol 10,(1), 2000.

[17]Spencer, M.G., Sanner, R.M., and Chopra, I., "Development of Neural Network Controller for Smart Structure Activated Rotor Blades", 39th AIAA/ASME/AHS Adaptive Structures Forum, Long Beach, CA, April 20-23, 1998.

[18]Spencer, M.G., Sanner, R.M., and Chopra, I., "Adaptive Neurocontroller for Vibration Suppression and Shape Control of a Flexible Beam", *Journal of Intelligent Material Systems and Structures*, Vol 9,(3), 1998.

[19]Johnson, W., "Self-Tuning Regulators for Multicyclic Control of Helicopter Vibration", NASA TP 1996, March 1982.

[20]Chopra, I., and McCloud, J.L., "Numerical Simulation Study of Open-Loop, Closed-Loop and Adaptive Multicyclic Control Systems", *Journal of the American helicopter Society*, Vol 38,(1), 1983.

[21]Roget, B., and Chopra, I., "Trailing-Edge Flap Control Methodology for Vibration Reduction of Helicopter with Dissimilar Blades", Proceedings of the 42nd AIAA/ASME/AHS Adaptive Structures Forum, Seattle, WA, April 16-18, 2001.

[22]Bir., G., Chopra, I., et al., "University of Maryland Advanced Rotorcraft Code (UMARC) Theory Manual", Technical report UM-AERO 94-18, Alfred Gessow Rotorcraft Center, University of Maryland, College Park, MD, July 1994.

[23]Gandhi, F., and Chopra, I., "Aeroelastic Analysis Methodology for Bearingless Main Rotor Helicopters", *Journal of the American Helicopter Society*, Vol 43,(1), Jan 1998.

[24]Bagai, A., and Leishman, J.G., "Rotor Free-Wake Modeling using a Pseudo-Implicit Technique - Including Comparisons with Experimental Data", *Journal of the American Helicopter Society*, Vol 40,(3), 1995.

[25]Gelb, A., Kasper, J.F., Nash, R.A., Price, C.F., and Sutherland, A.A., *Applied Optimal Estimation*, the M.I.T. press, 1974.